
Article

Not peer-reviewed version

Tunnel Fire Detection Method Based on Improved DS Evidence Theory

[Haiying Wang](#)*, Yuke Shi, Long Chen, Xiaofeng Zhang

Posted Date: 8 August 2024

doi: 10.20944/preprints202408.0573.v1

Keywords: Tunnel; Fire Detection; Multi-Sensor Data Fusion; DS Evidence Theory; PyroSim



Preprints.org is a free multidiscipline platform providing preprint service that is dedicated to making early versions of research outputs permanently available and citable. Preprints posted at Preprints.org appear in Web of Science, Crossref, Google Scholar, Scilit, Europe PMC.

Copyright: This is an open access article distributed under the Creative Commons Attribution License which permits unrestricted use, distribution, and reproduction in any medium, provided the original work is properly cited.

Disclaimer/Publisher's Note: The statements, opinions, and data contained in all publications are solely those of the individual author(s) and contributor(s) and not of MDPI and/or the editor(s). MDPI and/or the editor(s) disclaim responsibility for any injury to people or property resulting from any ideas, methods, instructions, or products referred to in the content.

Article

Tunnel Fire Detection Method Based on Improved DS Evidence Theory

Haiying Wang ^{1,*}, Yuke Shi ¹, Long Chen ¹ and Xiaofeng Zhang ²

¹ Key Laboratory of Road Construction Technology and Equipment of MOE, Chang'an University, Xi'an 710064, China; 2023125071@chd.edu.cn (Y.S.); 2023225125@chd.edu.cn (L.C.)

² Shaanxi Transportation Holding Group Co., Ltd., Xi'an 710075, China; 18192319988@139.com

* Correspondence: whying@chd.edu.cn

Abstract: Tunnel fires are generally detected using various sensors, including measuring temperature, CO concentration, and smoke concentration. To address the ambiguity and inconsistency in multi-sensor data, this paper proposes a tunnel fire detection method based on an improved Dempster-Shafer (DS) evidence theory for multi-sensor data fusion. To solve the problem of evidence conflict in DS theory, a two-level multi-sensor data fusion framework is adopted. The first level of fusion involves feature fusion of the same type of sensor data, removing ambiguous data to obtain characteristic data, and calculating the basic probability assignment (BPA) function through the feature interval. The second level fusion derives basic probability numbers from the BPA, calculates the degree of evidence conflict, normalizes to obtain the relative conflict degree, and optimizes the BPA using the trust coefficient. The classical DS evidence theory is then used to integrate and obtain the probability of tunnel fire occurrence. Different heat release rates, tunnel wind speeds, and fire locations are set, forming four fire scenarios. Sensor monitoring data under each simulation condition are extracted and fused using the improved DS evidence theory. The results show that the proposed improved DS evidence theory method detects the probability of fire occurrence in the four scenarios as 67.5%, 71.0%, 82.8%, and 83.5%, respectively, and identifies fire occurrence in approximately 2.4 seconds, an improvement of 64.7% to 70% over traditional methods. This demonstrates the feasibility and superiority of the proposed method, highlighting its significant importance in ensuring personnel safety.

Keywords: tunnel; fire detection; multi-sensor data fusion; DS evidence theory; PyroSim

1. Introduction

Multi-sensors play a crucial role in the detection of tunnel fires. Due to the unique environment of tunnels, the data collected by these sensors may contain ambiguous and conflicting information, leading to issues such as false alarms and missed detections of fires 1. Therefore, studying how to improve the accuracy of tunnel fire detection and the timeliness of fire discovery is of significant practical importance for tunnel safety.

Currently, common data fusion algorithms include artificial neural networks 2, Bayesian methods 3, Kalman filtering 4, and Dempster-Shafer (DS) evidence theory 5. Bayesian methods and DS evidence theory are often used to address multi-sensor data fusion issues 6. However, the Bayesian method's reliance on prior estimates can hinder its ability to accurately reflect changes in tunnel conditions, making it unsuitable for multi-sensor data fusion in tunnel fire scenarios 7. On the other hand, DS evidence theory is well-suited for situations where prior probabilities are unknown, allowing various sensor monitoring data to be integrated as evidence sources 8. Despite its advantages in handling uncertainty, DS evidence theory can produce paradoxical results when there is a high degree of evidence conflict. Solutions to the evidence conflict problem in DS evidence theory can be categorized into two types: altering fusion rules 9 and optimizing the BPA 10.

In terms of altering fusion rules, Xiao et al. 11 proposed a weighted combination method for conflict evidence in multi-sensor data fusion. This method adjusts the evidence weights by modifying the cosine similarity and confidence entropy to address the issue of highly conflicting evidence fusion. However, it essentially preprocesses the evidence without considering the characteristics of the evidence itself. Wang et al. 12 introduced an adaptive evidence fusion method based on power probability distance, but it uses a single evidence relation to represent and manage conflicts and uncertainties in the Internet of Things environment, failing to effectively address the impact of unreliable evidence sources on the fusion results. Hamda et al. 13 proposed an improved evidence combination method for representing conflict and uncertainty in data fusion to improve the accuracy of decision-making, mainly relying on the Hellinger distance. Murphy 14 simply averaged the mass functions and then applied the classical DS combination rule, without considering the correlation between pieces of evidence, and assigned the same weight to all evidence sources. Tang et al. 15 proposed a new method for uncertain information fusion based on a new evidence confidence coefficient, using the evidence distance in DS evidence theory to handle conflict and uncertain information fusion, but it introduces a single confidence function to determine the weights between evidence. Hu et al. 26 proposed a new confidence entropy method based on internal cross-information of evidence, which adjusts the comprehensive credibility of evidence and optimizes the evidence fusion process of the DS combination rule.

In terms of optimizing the BPA, Shahpari et al. 16 proposed a pixel-based transformation uncertainty measure based on BPA, but it has been proven in 17 that this measure does not satisfy certain properties and leads to paradoxes. Deng et al. 18 below introduced an improved DS evidence theory framework based on the Hellinger distance within uncertain intervals, which is more sensitive to changes in evidence. Xiao et al. 19 suggested a multi-sensor data fusion method based on evidence and information entropy confidence measure, using information entropy to assess the characteristics of the evidence itself. Qiao et al. 20 proposed a multi-sensor data fusion method based on evidence theory that assigns weights according to the degree of data deviation, demonstrating high fusion accuracy. Xiao 21 introduced the concept of evidence credibility measure and designed a hybrid multi-sensor data fusion method. Song et al. 22 presented a time evidence adaptive fusion method based on a negotiation strategy, constructing evidence set through cumulative time fusion, using probability distance to evaluate conflicts, and adapting the fusion of time evidence according to the degree of conflict. Zhao et al. 23 proposed a new distribution distance measure method to gauge the degree of conflict between pieces of evidence, introducing a modified information amount calculation method to evaluate the role of evidence and adjust evidence credibility. Zhou et al. 24 combined indirect conflict measurement indicators with evidence information measurement indicators for data fusion, addressing issues of high conflict and poor robustness. Wang et al. 25 developed a multi-attribute fusion algorithm based on fuzzy clustering and improved evidence theory, which uses fuzzy clustering for group measurement and then applies improved evidence theory for advanced fusion. Although these methods incorporate relationships between pieces of evidence and the characteristics of the evidence itself, they fuse the probabilities of target attributes collected by sensors for target recognition and fault diagnosis, failing to integrate the measurement results of the sensors. Moreover, using information entropy alone cannot comprehensively evaluate the characteristics of the evidence itself.

To more accurately measure the relationship between evidence and its intrinsic characteristics and to enhance the accuracy of data fusion, this paper proposes a tunnel fire detection method based on improved DS evidence theory for multi-sensor data fusion. To address the issue of DS evidence conflict, a two-level multi-sensor data fusion framework is employed. In the first level of fusion, feature fusion of the same type of sensor data is performed to eliminate ambiguous data and calculate the BPA. The second level of fusion addresses conflict issues by optimizing the BPA and then applying classical DS evidence theory for data fusion to obtain the probability of fire occurrence. This method aims to quickly and accurately detect tunnel fires under various fire conditions.

2. The Proposed Method

This section describes the relevant knowledge of DS evidence theory and explains the conflict issues in multi-sensor data fusion for tunnel fires. Finally, it proposes methods and steps for improving DS evidence theory.

2.1. Dempster-Shafer Evidence Theory

In DS evidence theory, the frame of discernment $\Theta = \{\theta_1, \theta_2, \dots, \theta_i, \dots, \theta_N\}$ consists of a finite set of mutually exclusive elements. 2^Θ denoted as the power set of the discursive framework, which is composed of 2^N elements, is represented as follows:

$$\begin{cases} m(\emptyset) = 0 \\ \sum_{A \subseteq \Theta} m(A) = 1 \\ m(A) \geq 0 \end{cases} \quad (1)$$

m is referred to as the Basic Probability Assignment (BPA) function, if $m(A) > 0$, $\{A\}$ is referred to as a proposition, and $m(A)$ denotes the degree of belief assigned to the proposition $\{A\}$.

In the frame of discernment Θ , $\forall A \subseteq \Theta$, If the function $Bel : 2^\Theta \rightarrow [0,1]$ satisfies:

$$Bel(A) = \sum_{B \subseteq A} m(B) \quad (2)$$

is said to $Bel(A)$ as the belief function of proposition $\{A\}$, which represents the likelihood that proposition $\{A\}$ is true.

In the frame of discernment Θ , $\forall A \subseteq \Theta$, If the function $Bel : 2^\Theta \rightarrow [0,1]$ satisfies:

$$Pl(A) = \sum_{B \cap A \neq \emptyset} m(B) \quad (3)$$

is said to $Pl(A)$ as the plausibility function of proposition $\{A\}$, which represents the likelihood that proposition $\{A\}$ is not false.

Defined $Pl(A)$ and $Bel(A)$ as the upper and lower bounds of the confidence in proposition $\{A\}$. The interval $[Bel(A), Pl(A)]$ represents the degree of uncertainty of the proposition, with the relationship between $Bel(A)$ and $Pl(A)$ illustrated in Figure 1.

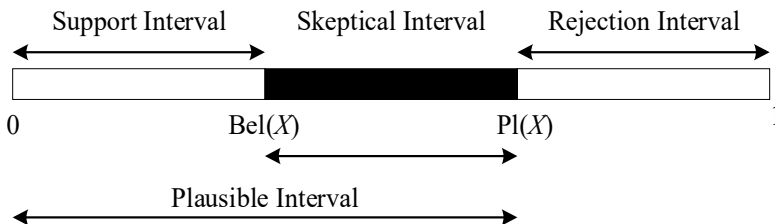


Figure 1. DS evidence theory confidence interval.

The combination rule of DS evidence theory involves merging multiple sources of evidence. Given two pieces of evidence with basic BPA m_1 and m_2 in the frame of discernment, the DS evidence theory fusion formula 27 for proposition $\{A\}$ is:

$$m(A) = \oplus = \begin{cases} 0 & X \cap Y = \Phi \\ \frac{\sum_{X \cap Y = A, \forall X, Y \subseteq U} m_1(X) \cdot m_2(Y)}{1-k} & X \cap Y \neq \Phi \end{cases} \quad (4)$$

where,

$$k = \sum_{X \cap Y = \Phi, \forall X, Y \subseteq U} m_1(X) \cdot m_2(Y) \quad (5)$$

when $k=1$, DS evidence theory is unable to fuse the evidence.

$$m(A) = \frac{\sum_{X \cap Y \cap Z \dots = A} m_1(X) m_2(Y) m_3(Z) \dots}{1-k} \quad A \neq \Phi, U \quad (6)$$

when there are three or more pieces of evidence, the combination rule of DS evidence theory is as follows:

$$k = \sum_{X \cap Y \cap Z \dots = \Phi} m_1(X) m_2(Y) m_3(Z) \dots \quad (7)$$

In the frame of discernment Θ , let A, B, and C represent the data from temperature sensors, CO sensors, and smoke sensors monitoring tunnel fires, respectively:

$$m_1 : m_1(A) = 0.75, m_1(B) = 0.15, m_1(C) = 0.1$$

$$m_2 : m_2(A) = 0, m_2(B) = 0.3, m_2(C) = 0.7$$

$$m_3 : m_3(A) = 0.8, m_3(B) = 0.15, m_3(C) = 0.05$$

Using the DS evidence theory combination rule, k was calculated to be 0.98975. The data fusion results $m(A)$, $m(B)$, and $m(C)$ are shown in Table 1.

Table 1. DS theory of evidence data fusion results.

Actual tunnel conditions	Multi-sensor fire BPA			Data fusion fire probability decision
	Temperature m1	CO m2	Soot concentration m3	Data fusion results
Fire conditions A	0.75	0	0.8	0
Fire warning conditions B	0.15	0.3	0.15	0.6585
Normal operating conditions C	0.1	0.7	0.05	0.3415

Relying solely on individual sensor data may result in temperature and smoke sensors indicating a higher likelihood of fire, while the CO sensor may indicate a normal state, leading to a paradox in data fusion based on Dempster-Shafer (DS) evidence theory. According to the data in Table 1, under fire conditions, the value of $m_2(\text{CO})$ is 0, which results in a post-fusion judgment of 0 for fire conditions. This causes a conflict in the DS evidence theory's judgment.

2.2. The Method for Improving D-S Evidence Theory

In the processing of data from similar sensors, the feature-level data fusion method can effectively eliminate ambiguous data and enhance the monitoring accuracy of environmental characteristics by similar sensors. For data from multiple types of sensors, decision-level fusion enables the complementary integration of multi-source data obtained from multiple sensors, thereby improving the accuracy of the monitoring results.

In tunnel fire detection, the raw data from temperature, CO concentration, and smoke concentration sensors are first subjected to feature extraction and correlation analysis of similar data. These features are then fused to form a comprehensive decision based on multi-source monitoring data, including temperature, CO concentration, and smoke concentration. On this basis, a decision-level fusion of multi-source data (temperature, CO concentration, smoke concentration) is performed to obtain the BPA of the evidence theory. The data fusion algorithm is then used to integrate these decision results, yielding the final fire probability. The proposed tunnel multi-sensor data fusion algorithm based on the improved DS evidence theory is illustrated in Figure 2.

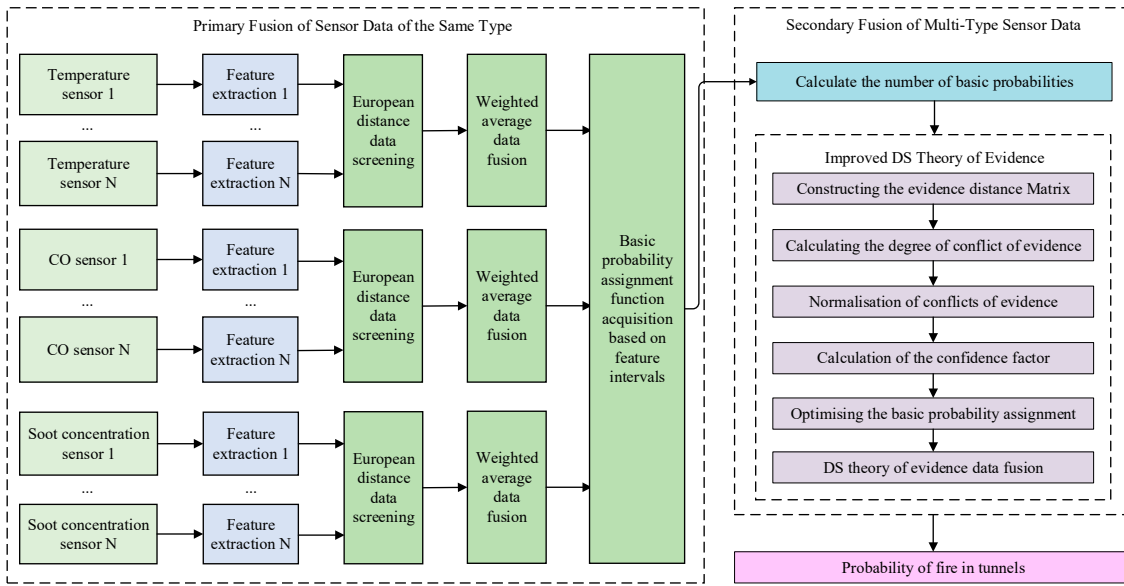


Figure 2. Multi-sensor data fusion algorithm based on improved DS evidence theory.

Step 1: Primary fusion of data from sensors of the same type to obtain BPA.

The key aspect of data fusion using Dempster-Shafer (DS) evidence theory is obtaining the BPA. Following the primary fusion process for similar sensor data, multi-sensor monitoring data are first collected, and invalid data are removed to obtain feature data. Then, a primary fusion of similar sensor data is performed. Finally, the BPA is preliminarily calculated based on the feature intervals.

Step 2: Secondary fusion of data from multiple types of sensors to obtain tunnel condition information.

The improved DS evidence theory addresses evidence conflict issues and yields the final fusion results of multi-sensor data. According to the secondary fusion process for multi-sensor data, the basic probability numbers are first derived from the BPA. Then, an evidence distance matrix is constructed to calculate the degree of conflict between pieces of evidence, and normalization is performed to obtain the relative conflict degree. Subsequently, the trust coefficients between pieces of evidence are calculated to further optimize the BPA. Finally, classical DS evidence theory is used to fuse the evidence and determine the tunnel conditions.

2.2.1. Primary Fusion of Data from Sensors of the Same Type

The process for obtaining the improved DS evidence theory BPA function for the fusion of data from sensors of the same type involves the following steps:

(1) Similar data screening based on Euclidean distance

To exclude anomalous data when calculating the BPA, this paper proposes a similar data screening algorithm based on Euclidean distance. The primary method involves measuring the similarity between data points by calculating the Euclidean distance between similar data. A smaller distance indicates a higher degree of similarity and greater data authenticity, while a larger distance indicates a lower degree of similarity and lesser data authenticity. Therefore, by calculating the

pairwise distances between all similar data points and setting an appropriate threshold, anomalies can be identified and excluded 29.

Let the number of sensors be n , and the distance between the collected like data $s_i = \{s_i \mid i = 1, 2, \dots, n\}$, The distance $d(s_i)$ 28 between s_i and other similar data excluding s_i can be expressed as:

$$\Delta d(i) = d(s_i) - d_m \quad (8)$$

$$d(s_i) = \left[\frac{1}{n} \sum_{j=1}^n (s_i - s_j)^2 \right]^{\frac{1}{2}}, i \neq j, i = 1, 2, \dots, n \quad (9)$$

The distance d_y of anomalous data is greater than the distance d_z of normal data. Therefore, the difference $\Delta d(i)$ between the distances of anomalous and normal data can be used to identify anomalous data. In the equation, d_m represents the median of $d(s_i)$.

Eliminating the magnitude of $\Delta d(i)$ by the following equation.

$$dw(s_i) = \frac{\Delta d(i)}{s_m} \quad (10)$$

where s_m represents the median of the set of sensor data of the same type s_i .

when $dw(s_i) \geq 0.02$, the sensor is considered to have a large error and should be rejected.

(2) Primary fusion of homogeneous sensor data using a weighted averaging method

If the weights are the same between sensors of the same type, then it is known that

$$\bar{x} = \frac{1}{n} \sum_{i=1}^n x_i \quad (11)$$

We defined \bar{x} as the fused value of data from the same type of sensors and $L(\bar{x})$ as the distance from \bar{x} to other sensors. When $L(\bar{x})$ reached its minimum value, \bar{x} was closest to the local multi-sensor monitoring result.

$$L(\bar{x}) = \sum_{i=1}^n (\bar{x} - x_i)^2 \quad (12)$$

derived that.

$$L(\bar{x}) = n\bar{x}^2 + \sum_{i=1}^n x_i^2 - 2\bar{x} \sum_{i=1}^n x_i \quad (13)$$

derivation on the left and right sides yields that

$$\frac{dL(\bar{x})}{d\bar{x}} = 2n\bar{x} - 2 \sum_{i=1}^n x_i \quad (14)$$

when $\bar{x} = \frac{1}{n} \sum_{i=1}^n x_i$, The minimum value of $L(\bar{x})$ is obtained, which corresponds to the average of the data from all sensors.

(3) Acquisition of BPA functions based on feature intervals

To monitor tunnel fire conditions in real-time, it is essential to collect three key types of data: carbon monoxide (CO) concentration, smoke concentration, and temperature. The identification

framework is $\Theta = \{A_1, A_2, \dots, A_{n-1}, A_n\}$, categorizes the tunnel fire status into three levels: {Normal Conditions, Warning Conditions, and Fire Conditions}.

Interval T represents the range within which the identification framework Θ is situated. This interval divides the n objects within the identification framework into n characteristic intervals T_i , $i=1,2,\dots,n$, which describe the range $[T_{iL}, T_{iR}]$ where the identification object A_i is located. The midpoint T_{iM} of each interval is set as the characteristic value for that feature interval.

$$T_{iM} = \frac{T_{iL} - T_{iR}}{2} \quad i=1,2,\dots,n \quad (15)$$

where T_{iL} represents the left boundary of the characteristic interval T_i , while T_{iR} represents the right boundary of the characteristic interval T_i .

Let $l(j)_i$ represent the distance between the sensor's measured value $a(j)$ and each characteristic value:

$$l(j)_i = |a(j) - T_{iM}| \quad i=1,2,\dots,n \quad (16)$$

Dividing $l(j)_i$ by the length of each characteristic interval yields the dimensionless distance $lw(j)_i$ between the sensor's measured value and each interval's characteristic value:

$$lw(j)_i = \frac{1}{T_{iL} - T_{iR}} l(j)_i \quad i=1,2,\dots,n \quad (17)$$

Taking the reciprocal of $lw(j)_i$ and normalizing it yields the probability assignment function $mass(j)_i$ and the basic probability number $mass(j)_i$ for the measured value $a(j)$.

$$mass(j)_i = \frac{1 / (lw(j)_i + C_0)}{\sum_{k=1}^n [1 / (lw(j)_k + C_0)]} \quad i=1,2,\dots,n \quad (18)$$

where C_0 is a constant.

According to equation (18), the closer the sensor's measured value is to the characteristic value T_{iM} of the interval, the larger $mass(j)_i$ becomes, indicating that $a(j)$ is closer to the identification object A_i . However, during a tunnel fire, some sensor measurements may exceed the right boundary T_{iR} of the characteristic interval T_i , causing $lw(j)_i$ to become too large and, consequently, $mass(j)_i$ to decrease, which moves $a(j)$ further away from the identification object A_i . Therefore, when calculating $mass(j)_i$, if $a(j)$ is too large, it should be replaced with $a(j)'$. Based on the characteristic interval T_i , this adjustment ensures that $a(j)$ remains close to the corresponding characteristic value T_{iM} .

$$a(j)' = T_{iM} + C_1 \quad (19)$$

where C_1 is a constant.

2.2.2. Secondary Fusion of Multi-Type Sensor Data

The improved DS evidence theory for multi-type sensor data fusion is applied to a secondary fusion process.

First, let the identification framework be $\Theta = \{A_1, A_2, A_3, \dots, A_n\}$, where A_n represents the n -Th condition of tunnel fire, and $E = \{E_1, E_2, E_3, \dots, E_m\}$ denotes the evidence set, with E_m being the m -Th piece of evidence related to the tunnel fire. The definition of the distance d_{ij} between evidence $mass_j$ and $mass_i$ is given by:

$$d_{ij} = e^{1-
$$E_i, E_j>} i, j = 1, 2, \dots, m \quad (20)$$$$

where

$$\langle E_i, E_j \rangle = \frac{\sum_{s=1}^m mass_i(A_s) mass_j(A_s)}{\sqrt{\sum_{s=1}^m mass_i^2(A_s)} \sqrt{\sum_{s=1}^m mass_j^2(A_s)}} \quad (21)$$

As d_{ij} approaches 1, it indicates a higher degree of mutual support between the pieces of evidence. Conversely, as d_{ij} approaches e, it signifies a higher level of conflict between the pieces of evidence. Based on this, an evidence distance matrix D can be constructed:

$$D = \begin{bmatrix} 1 & d_{12} & \dots & d_{1m} \\ d_{21} & 1 & \dots & d_{2m} \\ \vdots & \vdots & \ddots & \vdots \\ d_{m1} & d_{m2} & \dots & d_{mm} \end{bmatrix} \quad (22)$$

Defined $con(E_i)$ as the level of conflict between evidence.

$$con(E_i) = \sum_{i=1, i \neq j}^m d_{ij} \quad (23)$$

Normalize the evidence conflict degree to obtain the relative conflict degree of the evidence $in(E_i)$ 30.

$$in(E_i) = \frac{con(E_i)}{\sum_{j=1}^m con(E_j)} \quad (24)$$

Let $\lambda(E_i)$ be the trust coefficient of the evidence, representing the importance of evidence E_i and its influence on the fusion result. The definition of $\lambda(E_i)$ is:

$$\lambda(E_i) = [1 - in(E_i)] e^{-in(E_i)} \quad (25)$$

Let m_i be the original probability assignment function. The optimized probability assignment function $mass_i^*$ is:

$$mass_i^*(A_j) = \lambda(E_i) \cdot mass_i(A_j) \quad (26)$$

$$mass_i^*(X) = 1 - \lambda(E_i) \quad (27)$$

where $mass_i^*(X)$ denotes uncertainty.

In summary, the specific steps for improving the DS evidence theory for the secondary fusion of multi-sensor data in tunnels are as follows:

Firstly, an evidence distance matrix D is constructed to calculate the degree of conflict between the evidence and normalized to obtain the relative degree of conflict.

Secondly, calculates the trust coefficients between the evidence to optimize the BPA.

Finally, the evidence is fused using the classical DS theory of evidence.

3. Numerical Examples and Simulation Verification

This section evaluates and simulates the proposed method based on the improved DS evidence theory to verify its feasibility and effectiveness.

3.1. Improved DS Evidence Theory

To validate the effectiveness of the proposed improvement, sensor monitoring data from Section 2.1 are used to compare the proposed improved algorithm with the methods developed by Dempster-Shafer 31, Yanger 32, Sun 33, and Murphy 14. The fusion results are shown in Table 2. and the comparison of the fusion results is illustrated in Figure 3.

Table 2. Data fusion results of five algorithms.

	Fire conditions m(A)	Fire warning conditions m(B)	Normal operating conditions m(C)	Uncertainty m(X)
DS	0	0.65850	0.34150	
Yager	0	0.00675	0.01050	0.98275
Sun	0.24746	0.10254	0.13921	0.51079
Murphy	0.34536	0.04751	0.25606	0.35107
This paper	0.50247	0.13253	0.16821	0.19679

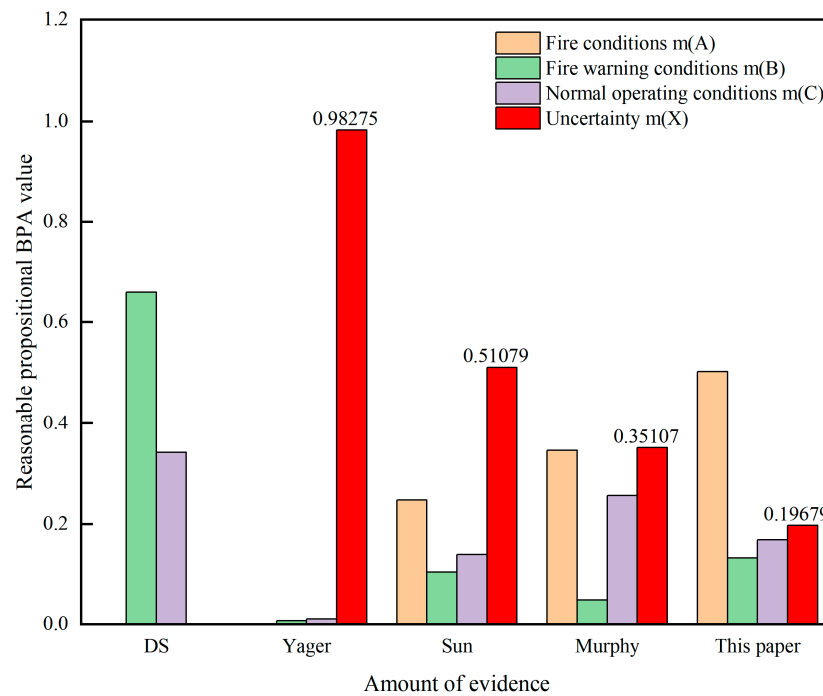


Figure 3. Comparison of data fusion results for five algorithms.

From Table 3. it can be observed that under fire condition A, when $m_1 = 0.8$, $m_2 = 0$, and $m_3 = 0.7$, the BPA $m(A)$ for Yanger's method is 0, which results in a paradox. In contrast, the BPA for fire conditions in this paper is 0.50247, indicating the detection of a fire. When dealing with different

types of conflicting evidence, classical DS and Yager's fusion methods lead to contradictions with the actual facts. Although the method proposed by Sun et al. points to the correct result, it exhibits a higher degree of uncertainty. Therefore, traditional DS fusion rules may fail or mismatch the actual tunnel fire conditions when confronted with conflicting evidence. This paper addresses the problem of evidence conflict by reducing the proportion of conflicting evidence, gradually decreasing the number of conflicting evidence, and increasing the amount of valid evidence, thus minimizing the uncertainty interval and enhancing reliability. The improved DS evidence theory fusion algorithm proposed in this paper provides more accurate results in handling evidence and conflicting evidence, demonstrating the rationality and effectiveness of the proposed method.

3.2. The Proposed Holistic Approach

To further demonstrate the feasibility and effectiveness of the data fusion method, this subsection applies the proposed improved DS evidence theory data fusion method to tunnel fire detection.

In tunnel fire detection, temperature sensors, CO sensors, and smoke sensors are commonly used to monitor fires [34]. The PyroSim software, based on Fire Dynamics Simulator (FDS) and Computational Fluid Dynamics [35], can simulate large-scale slow-moving vortices and accurately obtain critical parameters such as fire heat release, fire smoke, CO concentration, and temperature.

The fire simulation process using PyroSim is illustrated in Figure 4. First, a comprehensive tunnel geometric model is created, including elements such as lining, vehicles, and ventilation systems, to accurately describe the internal structure of the tunnel. Next, multiple sensors, including temperature, CO, and smoke sensors, are installed to enable real-time monitoring of the fire scene. The heat release rate is determined based on the actual fire conditions. Subsequently, a tunnel fire simulation model is established, and simulation parameters such as temperature and velocity are set to realistically simulate the fire situation. Finally, FDS is run to perform the fire simulation and obtain multi-sensor monitoring data.

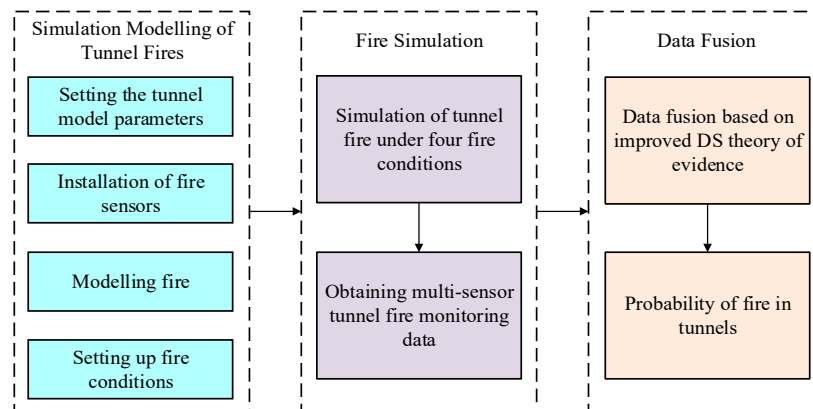


Figure 4. Tunnel fire simulation process.

3.2.1. Simulation Model

(1) Establishing the tunnel geometric model

The tunnel geometric model is constructed with the following specifications: a height of 8.5 meters, a width of 14.5 meters, and a length of 600 meters. The tunnel is lined with 31 concrete walls forming the lining and surrounding rock structure. The wall material has a density of 2280.0 kg/m^3 , a specific heat capacity of $1.04 \text{ kJ/(kg}\cdot\text{K)}$, and a thermal conductivity of $1.8 \text{ W/(m}\cdot\text{K)}$. In consideration of practical scenarios, the dimensions of the vehicles are set as follows: width 2.4 meters, height 2.5 meters, and length 7 meters. The fire materials carried by large trucks are wood and plastic. In the tunnel model, a blue square on the top represents the jet fan, which has an outlet area of 1.21 m^2 and

a wind speed of 27.9 m/s. These parameters are used to establish the tunnel geometric model, with the specific structure illustrated in Figure 5.

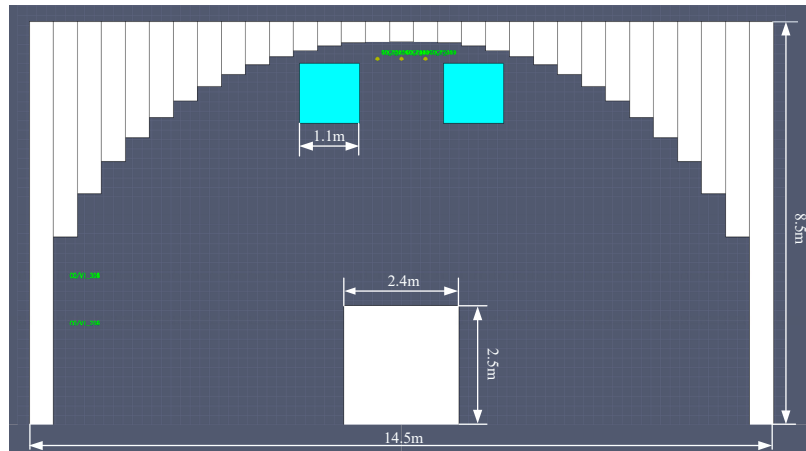


Figure 5. Tunnel geometric model.

(2) Installation of fire monitoring equipment

A 3x3 sensor matrix is arranged on the tunnel ceiling, with each matrix containing 3 temperature sensors, 3 CO sensors, and 3 smoke sensors. The distance between adjacent sensor matrices is 10 meters. Additionally, pairs of smoke sensors are installed on the right side of the tunnel at heights of 2 meters and 3 meters from the ground, with a distance of 100 meters between adjacent pairs. The specific arrangement of the sensors is illustrated in Figure 6.

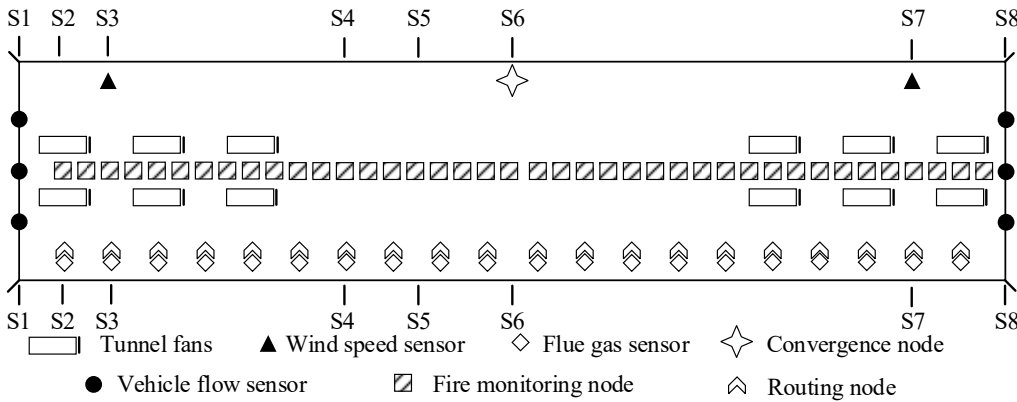


Figure 6. Tunnel fire monitoring sensor layout.

(3) Establishing the fire model

The tunnel accommodates various vehicle types, including large trucks and small cars, so the corresponding heat release rates are set to 20 MW for large trucks and 5 MW for small cars. During a fire, higher wind speeds result in faster smoke spread and greater disruption to the smoke layer, increasing danger. Based on traffic volume survey data, the simulation wind speed is set to 2.5 m/s, with 3 m/s and zero wind speed used as control conditions. The tunnel is set with a pressure of 94.5 kPa, an initial temperature of 20°C, an initial CO concentration of 42 cm³/m³, and an initial smoke concentration K of 0.004 m⁻¹.

When a fire occurs at the midpoint of the tunnel, the distance for personnel evacuation to the exits is maximized, which is unfavorable for evacuation; simultaneously, the tunnel fan is located farthest from the fire source, making smoke control less effective. In Figure 7, ignition point 1 is located at the midpoint of the tunnel, representing the main fire condition, while ignition point 2 is near the entrance fan, serving as the control condition. The farther the sensor is from the ignition

point, the more challenging it is to monitor the tunnel fire. Therefore, the distance between the ignition point and the downstream sensor matrix is set to 7.5 meters.

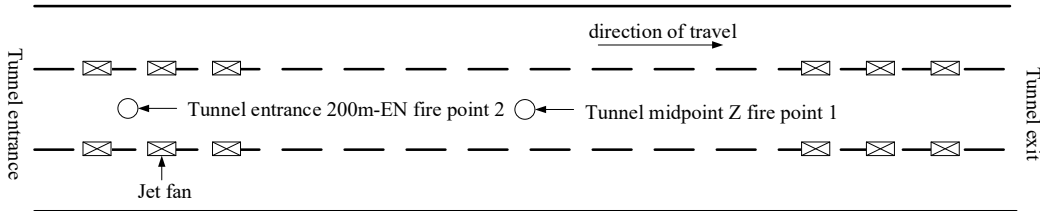


Figure 7. Tunnel ignition point locations.

Based on the established fire conditions, with other fire conditions remaining consistent, four types of tunnel fire conditions are set as shown in Table 3.

Table 3. Tunnel fire conditions.

Condition Number	Ignition Point L	Heat Release Rate (MW)	Wind Speed (m/s)
LZ-R5-S2.5	Tunnel Midpoint-Z	5	2.5
LZ-R20-S0	Tunnel Midpoint-Z	20	0
LZ-R20-S2.5	Tunnel Midpoint-Z	20	2.5
LEN-R20-S3	Tunnel Entrance 200m-EN	20	3

3.2.2. Tunnel Fire Simulation

Based on the tunnel fire conditions set in Section 3.2.1, simulations are conducted in PyroSim. Using the condition LZ-R5-S2.5 as an example, the multi-sensor monitoring data for tunnel fires are obtained. The monitoring data for temperature sensors, smoke sensors, and CO sensors in the fire monitoring nodes are shown in Table 4.

Table 4. Multi-sensor monitoring data for tunnel fire condition LM-R5-S2.5.

Time(s)	Temperature (°C)			Soot concentration (m⁻¹)			CO concentration (cm³/m³)		
	1	2	3	Gas 1	Gas 2	Gas 3	CO_1	CO_2	CO_3
0.6	20	20	20	0.0040	0.0040	0.0040	42	42	42
1.2	20.01	20.01	20.01	0.0040	0.0040	0.0040	42	42	42
1.8	20.04	20.04	20.04	0.0040	0.0040	0.0040	42	42	42
2.4	20.23	20.23	20.23	0.0040	0.0040	0.0040	42	42	42
3	50	20.55	20.55	0.0040	0.0040	0.0040	42	42	42
3.6	28.95	28.99	28.9	0.0070	0.0070	0.0070	51	51	51
4.2	46.22	46.7	46.22	0.0707	0.0706	0.0708	48	48	48
4.8	54.75	55.73	54.75	0.0597	0.0595	0.0599	43	43	43
5.4	62.03	63.39	62.03	0.0588	0.0587	0.0589	44	44	44
6	67.59	68.72	67.59	0.0591	0.0591	0.0591	44	44	44
6.6	66.65	67.46	66.65	0.0624	0.0624	0.0625	43	43	43
7.2	72.59	73.28	72.59	0.0394	0.0396	0.0392	44	44	44
7.8	78.1	78.77	78.1	0.0569	0.0587	0.0551	43	43	43
8.4	82.01	82.82	75	0.0604	0.0598	0.0610	42	42	42
9	82.05	82.7	82.05	0.0662	0.0655	0.0669	42	42	42
9.6	79.91	80.46	79.91	0.0719	0.0724	0.0715	42	42	42
10.2	79.08	79.77	79.08	0.0525	0.0539	0.0512	43	42	44
10.8	75.8	77.15	75.8	0.0536	0.0518	0.0554	43	42	43

3.2.3. Tunnel Fire Simulation Data Fusion

Based on the "Highway Tunnel Ventilation Design Specifications" and relevant design standards for tunnel engineering, the characteristic intervals for temperature, smoke concentration, and CO concentration are categorized as shown in Table 5.

Table 5. Feature interval classification.

State Space	Normal conditions	Fire warning Conditions	Fire conditions
Temperature range (°C)	0~40	40~55	55~100
Soot concentration range (m^{-1})	0.0000~0.0075	0.0075~0.0120	0.0120~0.0750
CO concentration interval (cm^3/m^3)	0.00~107.50	107.50~150.00	150.00~350.00

The primary fusion data of sensor readings under four different operating conditions, combined with Table 5, were used to calculate the probability assignment functions as shown in Table 6, according to Equations (18) and (19).

Table 6. Probability assignment functions for operating condition LM-R5-S2.5.

Time (s)	Temperature $mass_1$			Soot concentration $mass_2$			CO concentration $mass_3$		
	A	B	C	A	B	C	A	B	C
0.6	0.60	0.17	0.24	0.91	0.03	0.06	0.85	0.05	0.10
1.2	0.60	0.17	0.24	0.91	0.03	0.06	0.85	0.05	0.10
1.8	0.60	0.17	0.24	0.91	0.03	0.06	0.85	0.05	0.10
2.4	0.60	0.16	0.23	0.91	0.03	0.06	0.85	0.05	0.10
3	0.61	0.16	0.23	0.91	0.03	0.06	0.85	0.05	0.10
3.6	0.90	0.05	0.05	0.42	0.29	0.29	0.95	0.02	0.03
4.2	0.08	0.82	0.10	0.05	0.03	0.92	0.91	0.03	0.06
4.8	0.17	0.41	0.42	0.04	0.02	0.94	0.87	0.05	0.09
5.4	0.14	0.22	0.64	0.04	0.02	0.94	0.87	0.04	0.08
6	0.09	0.13	0.78	0.04	0.02	0.94	0.87	0.04	0.09
6.6	0.10	0.14	0.76	0.04	0.03	0.93	0.86	0.05	0.09
7.2	0.05	0.06	0.89	0.02	0.01	0.97	0.87	0.04	0.08
7.8	0.01	0.01	0.98	0.03	0.02	0.95	0.86	0.05	0.09
8.4	0.04	0.05	0.91	0.04	0.03	0.94	0.85	0.05	0.10
9	0.04	0.05	0.91	0.04	0.03	0.93	0.85	0.05	0.10
9.6	0.03	0.03	0.95	0.05	0.03	0.92	0.85	0.05	0.10
10.2	0.02	0.02	0.96	0.02	0.02	0.96	0.87	0.05	0.09
10.8	0.02	0.02	0.97	0.03	0.02	0.96	0.86	0.05	0.09

The probability assignment function is optimized using Equations (26) and (27), and the probability assignment function for unknown conditions is calculated. Combining the optimized probability assignment function with Equation (6), the probabilities of normal operation, fire warning, fire state, and unknown state under various tunnel conditions are determined, as shown in Table 7.

Table 7. Tunnel states computed using improved DS evidence theory for fire condition LM-R5-S2.5.

Time (s)	Normal conditions	Fire warning conditions	Fire conditions	Uncertainty
0.6	71.30%	4.20%	7.00%	17.50%
1.2	71.30%	4.20%	7.00%	17.50%
1.8	71.30%	4.20%	7.00%	17.50%
2.4	71.50%	4.00%	6.90%	17.60%
3	71.60%	4.00%	6.80%	17.60%

3.6	69.90%	5.80%	6.10%	18.20%
4.2	25.90%	21.30%	27.90%	24.90%
4.8	22.80%	12.20%	42.90%	22.10%
5.4	19.00%	6.60%	53.70%	20.70%
6	16.00%	4.10%	60.00%	19.90%
6.6	16.30%	4.80%	58.80%	20.10%
7.2	13.20%	2.10%	65.30%	19.40%
7.8	11.70%	1.30%	67.90%	19.10%
8.4	13.20%	2.40%	65.00%	19.40%
9	13.30%	2.40%	64.80%	19.50%
9.6	13.20%	2.00%	65.60%	19.20%
10.2	11.90%	1.50%	67.50%	19.10%
10.8	12.00%	1.50%	67.50%	19.00%

For the different conditions mentioned above, the simulation results using the same method are shown in Figure 8.

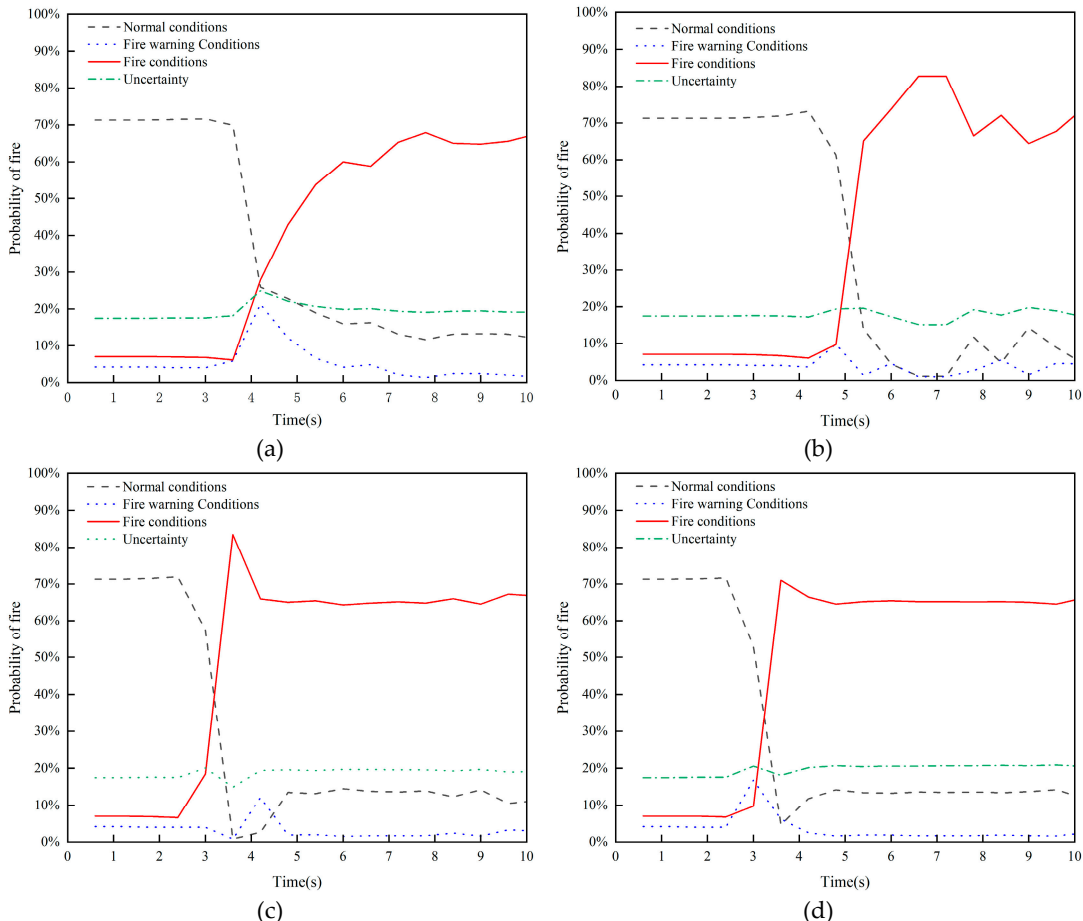


Figure 8. Probability curves of tunnel fire occurrence under different conditions. (a) LZ-R5-S2.5. (b) LZ-R20-S0. (c) LZ-R20-S2.5. (d) LEN-R20-S3.

The fire occurrence probabilities under various conditions are analyzed, and the resulting curves for the four types of fire conditions are shown in Figure 9.

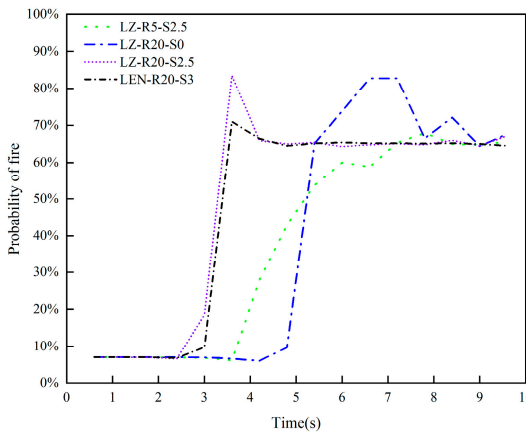


Figure 9. Comparison of tunnel fire occurrence probability curves under four conditions.

Based on the multi-sensor monitoring data and fusion results for tunnel fires under different conditions, the following conclusions can be drawn:

A higher heat release rate and wind speed make it easier to detect tunnel fires. The fire condition LZ-R5-S2.5, with a lower heat release rate, presents the greatest challenge for fire detection. The improved DS evidence theory multi-sensor data fusion algorithm reached a conclusion of fire occurrence at 7.2 seconds based on changes in tunnel temperature and smoke concentration. Thus, the improved DS evidence theory multi-sensor data fusion algorithm demonstrates good fusion performance under zero wind speed and low heat release rate conditions.

The probabilities of tunnel fire occurrence under the four conditions are 67.5%, 82.8%, 83.5%, and 71%, respectively. This indicates that the proposed method has a high monitoring accuracy.

The comparison results of the improved DS evidence theory multi-sensor fusion algorithm with those of Sun and the original methods are shown in Figure 10.

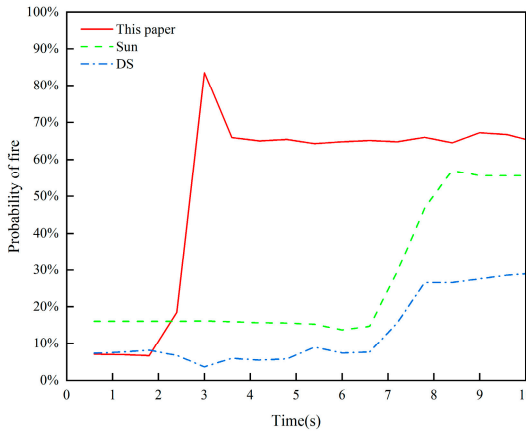


Figure 10. Comparison of fire state prediction curves.

Figure 10. presents the fire occurrence probabilities for various methods. Compared to other methods, the approach proposed in this paper improves fire detection accuracy by 5% to 10.2%, reduces the time required to identify a fire to approximately 2.4 seconds (64.7% to 70% improvement over other methods), and simultaneously enhances both the timeliness and accuracy of monitoring. This demonstrates its feasibility and effectiveness in multi-sensor data fusion.

4. Conclusion

This paper proposes a multi-sensor data fusion algorithm based on improved DS evidence theory, which effectively monitors the environment and fire conditions within a tunnel, significantly enhancing the accuracy and efficiency of monitoring.

Propose a multi-sensor data fusion algorithm based on an improved DS evidence theory, employing a two-level fusion architecture. Initially, the data collected by different sensors is screened to eliminate inaccurate data. Subsequently, primary fusion is performed on data from sensors of the same type. Next, BPA functions for fire, fire warning, and normal operating conditions are extracted from the results of the primary fusion. Evidence conflicts are treated as a manifestation of uncertainty, and BPA functions are optimized. Finally, the optimized evidence is fused using DS evidence theory to achieve an accurate assessment of the tunnel's operational status.

To address the conflict issue in DS evidence theory, an improved DS evidence theory fusion algorithm is proposed. Comparisons with other data fusion algorithms show that the proposed method achieves a smaller uncertainty interval (0.19679). By making full use of tunnel fire data information, the fusion results exhibit higher credibility.

The proposed multi-sensor data fusion algorithm was validated using multi-sensor monitoring data. The results indicate that the method consistently achieves a fire detection probability of no less than 65% across four different operational conditions. Compared to other research methods, the proposed algorithm offers faster analysis speeds and makes more comprehensive use of tunnel environment information. This demonstrates its potential for practical application in tunnel safety monitoring systems and suggests that it could enhance the early warning capabilities for tunnel fires.

Author Contributions: H.W. designed the experiment; Y.S. performed the experiments and wrote the manuscript; L.C. analyzed the experimental data; X.Z. supervised version of the manuscript. All authors have read and agreed to the published version of the manuscript.

Funding: This research was funded by the Transport Research Project of the Department of Transport of Shaanxi Province. (Grant nos. 21-04X).

Institutional Review Board Statement: Not applicable.

Informed Consent Statement: Not applicable.

Data Availability Statement: Not applicable.

Acknowledgments: The authors greatly appreciate the reviews, the suggestions from reviews, and the editor's encouragement.

Conflicts of Interest: The author declare no conflict of interest.

References

1. Yu, L.F. Tunnel Fire Monitoring and Alarm Technology Based on Multi-Sensor Data Fusion. *Tunn. Constr.* **2022**, *42*, 261–266. <https://doi.org/10.3973/j.issn.2096-4498.2022.S2.032>
2. Li, N. The Construction of a Fire Monitoring System Based on Multi-Sensor and Neural Network. *Int. J. Inf. Technol. Syst. Approach* **2023**, *16*: 1-12. <https://doi.org/10.4018/IJITSA.326052>
3. Wu, P.; Imbiriba, T.; Elvira, V.; Closas, P. Bayesian data fusion with shared priors. *IEEE Tran. Signal Process.* **2023**, *72*, 275–288. <https://doi.org/10.1109/TSP.2023.3343564>
4. Li, L.; Li, A.; Yan, Y.J. Analysis of data fusion method for multiple temperature sensors based on improved Kalman filtering. *Electron. Technol.* **2024**, *53*, 214–215. <https://doi.org/10.3969/j.issn.1000-0755.2024.03.087>
5. Huang, Z.Y.; Lin, R.M.; Liu, H.; Zhu, J.Y.; Li, J.K. A multi-source network security data fusion model based on DS evidence theory. *Mod. Electron. Technol.* **2024**, *47*, 115–121. <https://doi.org/10.16652/j.issn.1004-373x.2024.07.020>
6. Xiang, X.J.; Li, K.H.; Huang, B.Q.; Cao, Y. A multi-sensor data-fusion method based on cloud model and improved evidence theory. *Sensors* **2022**, *22*, 5902. <https://doi.org/10.3390/s22155902>
7. Zhang, F.X.; Zhang, L.M.; Liu, Z.Y.; Meng, F.Z.; Wang, X.S.; Wen, J.H.; Gao, L.Y. An Improved Dempster-Shafer Evidence Theory Based on the Chebyshev Distance and Its Application in Rock Burst Prewarnings. *ASCE-ASME J. of Risk Uncertain. Eng. Syst. Part A-Civ. Eng.* **2024**, *10*, 04023055. <https://doi.org/10.1061/AJRUA6.RUENG-1201>
8. Ye, F.; Chen, J.; Li, B.Y. Improvement of DS evidence theory for multi-sensor conflicting information. *Symmetry-Basel* **2017**, *9*, 69. <https://doi.org/10.3390/sym 9050069>
9. Du, Y.W.; Zhong, J.J. Generalised combination rule for evidential reasoning approach and Dempster-Shafer theory of evidence. *In. Sci.* **2021**, *547*, 1201–1232. <https://doi.org/10.1016/j.ins.2020.07.072>
10. Shi, X.; Liang, F.; Qin, P.J.; Yu, L.; He, G.J. A Novel Evidence Combination Method Based on Improved Pignistic Probability. *Entropy* **2023**, *25*, 948. <https://doi.org/10.3390/e25060948>

11. Xiao, F.Y.; Qin, B.W. A weighted combination method for conflicting evidence in multi-sensor data fusion. *Sensors* **2018**, *18*, 1487. <https://doi.org/10.3390/s18051487>
12. Wang, J.; Zhu, J.W.; Song, Y.F. A self-adaptive combination method in evidence theory based on the power pignistic probability distance. *Symmetry-Basel* **2020**, *12*, 526. <https://doi.org/10.3390/sym12040526>
13. Hamda, N.E.; Hadjali, A.; Lagha, M. Multisensor Data Fusion in IoT Environments in Dempster-Shafer Theory Setting: an Improved Evidence Distance-Based Approach. *Sensors* **2023**, *23*, 5141. <https://doi.org/10.3390/s23115141>
14. Murphy, C. K. Combining belief functions when evidence conflicts. *Decis. Support Syst.* **2000**, *29*, 1–9. [https://doi.org/10.1016/s0167-9236\(99\)00084-6](https://doi.org/10.1016/s0167-9236(99)00084-6)
15. Tang, Y.C.; Wu, S.H.; Zhou, Y.; Huang, Y.B.; Zhou, D.Y. A new reliability coefficient using betting commitment evidence distance in Dempster-Shafer evidence theory for uncertain information fusion. *Entropy* **2023**, *25*, 462. <https://doi.org/10.3390/e25030462>
16. Shahpari, A.; Seyedin, S.A. Using mutual aggregate uncertainty measures in a threat assessment problem constructed by Dempster-Shafer network. *IEEE Tran. Syst. Man Cybern. Syst.* **2015**, *45*, 877–886. <https://doi.org/10.1109/TSMC.2014.2378213>
17. Abellán, J.; Bosse, E. Drawbacks of uncertainty measures based on the pignistic transformation. *IEEE Tran. Syst. Man Cybern. Syst.* **2016**, *48*, 382–388. <https://doi.org/10.1109/TSMC.2016.2597267>
18. Deng, Z.; Wang, J.Y. Measuring total uncertainty in evidence theory. *Int. J. Intell. Syst.* **2021**, *36*, 1721–1745. <https://doi.org/10.1002/int.22358>
19. Xiao, F. Multi-sensor data fusion based on the belief divergence measure of evidences and the belief entropy. *Inf. Fusion* **2019**, *46*, 23–32. <https://doi.org/10.1016/j.inffus.2018.04.003>
20. Qiao, S.H.; Fan, Y.S.; Wang, G.F.; Zhang, H.Y. Multi-sensor data fusion method based on improved evidence theory. *J. Mar. Sci. Eng.* **2023**, *11*, 1142. <https://doi.org/10.3390/jmse11061142>
21. Xiao, F. Evidence combination based on prospect theory for multi-sensor data fusion. *ISA Tran.* **2020**, *106*, 253–261. <https://doi.org/10.1016/j.isatra.2020.06.024>
22. Song, Y.F.; Zhu, J.W.; Lei, L.; Wang, X.D. Self-adaptive combination method for temporal evidence based on negotiation strategy. *Sci. China Inf. Sci.* **2020**, *63*, 1–13. <https://doi.org/10.1007/s11432-020-3045-5>
23. Zhao, K.Y.; Sun, R.T.; Li, L.; Hou, M.M.; Yuan, G.; Sun, R.Z. An improved evidence fusion algorithm in multi-sensor systems. *Appl. Intell.* **2021**, *51*, 7614–7624. <https://doi.org/10.1007/s10489-021-02279-5>
24. Zhou, K.Y.; Lu, N.Y.; Jiang, B. Information fusion-based fault diagnosis method using synthetic indicator. *IEEE Sens. J.* **2023**, *23*, 5124–5133. <https://doi.org/10.1109/JSEN.2023.3238344>
25. Wang, W.Q.; Yan, Y.; Zhang, R.D.; Wang, Z.; Fan, Y.Q.; Yang, C.J. Multi-attribute fusion algorithm based on improved evidence theory and clustering. *Sensors* **2019**, *19*, 4146. <https://doi.org/10.3390/s19194146>
26. Hu, Z.T.; Su, Y.J.; Hou, W.; Ren, X. Multi-sensor data fusion method based on divergence measure and probability transformation belief factor. *Appl. Soft. Comput.* **2023**, *145*, 110603. <https://doi.org/10.1016/j.asoc.2023.110603>
27. Chu, L.Y.; Wang, M.Y.; Chen, X.Q. Risk assessment of maritime supply chain based on improved DS evidence theory and Bayesian network. *Supply Chain Manag.* **2024**, *5*, 82–96. <https://doi.org/10.19868/j.cnki.gylgl.2024.02.006>
28. Peng, D.G.; Duan, R. J.; Wang, D.H. Two-tier fusion-based multi-sensor data fusion algorithm research. *Instrum. Tech. Sens.* **2024**, *87*-93. <https://doi.org/10.3969/j.issn.1002-1841.2024.01.016>
29. Zhou, E.F.; Ma, J.; Zhou, Y.J.; Wang, Q.Q.; Chen, B.H. Multi-sensor data fusion algorithm based on D-S evidence theory. *J. Chin. Comput. Syst.* **2022**, *43*, 795–800. <https://doi.org/10.20009/j.cnki.21-1106/TP.2020-0967>
30. Wu, L.S.; Chen, L.; Hao, X.R. Multi-Sensor Data Fusion Algorithm for Indoor Fire Early Warning Based on BP Neural Network. *Information* **2021**, *12*, 59. <https://doi.org/10.3390/info12020059>
31. Dempster, A.P. Upper and Lower Probabilities Induced by a Multi-valued Mapping. *Ann. Math. Stat.* **1967**, *38*, 325–339. <https://doi.org/10.1214/aoms/1177698950>
32. Yager, R.R. On the Dempster-Shafer framework and new combination rules. *Information sciences. Inf. Sci.* **1987**, *41*, 93–137. [https://doi.org/10.1016/0020-0255\(87\)90007-7](https://doi.org/10.1016/0020-0255(87)90007-7)
33. Sun, Q.; Ye, X.Q.; Gu, W.K. A New Combination Rules of Evidence Theory. *Acta Electronica Sin.* **2000**, *28*, 117–119. <https://doi.org/10.3321/j.issn:0372-2112.2000.08.036>

Disclaimer/Publisher's Note: The statements, opinions and data contained in all publications are solely those of the individual author(s) and contributor(s) and not of MDPI and/or the editor(s). MDPI and/or the editor(s) disclaim responsibility for any injury to people or property resulting from any ideas, methods, instructions or products referred to in the content.